Journal of Alloys and Compounds 509 (2011) 8223–8227

Contents lists available at ScienceDirect

Journal of Alloys and Compounds

journal homepage: www.elsevier.com/locate/jallcom

Transition metal modified bulk $BiFeO_3$ with improved magnetization and linear magneto-electric coupling

Venkata Sreenivas Puli*, A. Kumar, N. Panwar[1], I.C. Panwar, R.S. Katiyar

Department of Physics and Institute for Functional Nanomaterials, University of Puerto Rico, San Juan, PR 00936, USA

ARTICLE INFO

Article history:
Received 22 April 2011
Accepted 20 May 2011
Available online 1 June 2011

Keywords:
Multiferroics
Magnetoelectric coefficient

ABSTRACT

At present $BiFeO_3$ (BFO) is the most attractive and sole example, which possesses low magnetization value, high leakage current and low polarization in ceramic form. Single-phase room temperature multiferroics are rare in nature. This paper deals with the improved magnetic and observed linear magneto-electric coupling in Co and Sm co-doped $BiFeO_3$ ceramics synthesized by sol–gel process at low temperature ~600 °C. As synthesized $Bi_{0.9}Sm_{0.10}Fe_{0.95}Co_{0.05}O_3$ (BSFCO) showed high impurities phases (20%) over wide range of calcination temperatures. Impurity phases reduced drastically from 20% to 5% after leaching with nitric acid. However the electrical and the magnetic properties were almost the same for both phases. Well-defined magnetic hysteresis with high magnetic moment was found at room temperature. Ferroelectric polarization studies demonstrated similar values and shape as reported in literature for the pure bulk BFO. Linear magneto-electric (ME) coupling and weak ME coefficient (α) ~ 0.6 e−10 s m^{-1} were observed in the co-doped BFO. The origin of the strong ferromagnetic property in our samples may be due to the presence of rare earth and transition metal ions at the lattice sites of BFO or due to impurity phase, since we have not seen any change in magnetization with reduction of impurity phase the later effect is more unlikely.

1. Introduction

There is a tremendous growing interest since last decade towards mutlferroic materials which exhibit ferromagnetism, ferroelectricity and/or ferroelasticity property simultaneously [1]. Compound like, $BiMnO_3$, $BiFeO_3$ (BFO) and some rare-earth magnites (e.g., $RMnO_3$ with R = Er, Ho, Lu, Tb, Yb and Y) have been widely studied since 1950s as multiferroics [3]. Most multiferroics are also magnetoelectric (ME), which is induction of magnetization by means of an electric field or induction of polarization by means of magnetic field [1]. BFO is a well-known room temperature multiferroic material. It has a rhombohedrally (R3c) distorted ABO_3 perovskite structure in its ferroelectric state with a high Curie temperature (~830 °C) and exhibiting antiferromagnetic behavior (weak ferromagnetism) with relatively high Neel temperature (~380 °C) [5]. However, the reduction in particle size considerably reduces Neel temperature and which is correlated to lattice volume contraction [6]. BFO shows G-type antiferromagnetic structural behavior with modulated spiral spin structure with long periodicity of 62 nm in the unit cell [7]. Even though comprehensive studies were conducted on BFO in early 1960s, not much was reported on ferroelectric properties, initially due to its higher conductivity and also due to the presence of impurity phases. Synthesis of phase pure BFO in bulk and as well as nanoparticles is a challenging task, due to narrow temperature range phase stabilization and kinetics of phase formation in the Bi_2O_3 and Fe_2O_3 systems [8–10]. High leakage current in $BiFeO_3$ is attributed to existence of smaller number Fe^{+2} ions, oxygen vacancies [12], and inferior ferroelectric behavior that are due to impure phase like $Bi_2Fe_4O_9$, $Bi_{12}(Bi_{0.5}Fe_{0.5})O_{19.5}Bi_{25}FeO_{40}$, and $Bi_{25}FeO_{40}$ [10,11]. The oxygen vacancies arise due to Bi deficiency with its highly volatile nature and doping with rare earth elements will suppress the oxygen vacancies due to Bi deficiency [1]. Doping with isovalent lanthanide elements at A-site cation, i.e. Bi in BFO leads to improved ferroelectric properties [7]. Mutliferroic materials are utilized in manufacturing multifunctional devices [1–10]. Magnetic perovskite oxides like $BiFeO_3$, $YMnO_3$, were widely studied in thin film forms in which $BiFeO_3$ is a promising candidate in nanoscale devices, such as high density magnetically recorded ferroelectric memories [12]. Magnetic properties in BFO were further increased by substitution of either Bi^{+2} with Tb, Nd, Sm, Gd [13–16] or Fe^{+3} ions with Cr, Co, Mn, Sc doping [12,17–22,25]. Leakage current is reduced in La doped BFO thin films and is attributed to phase stability and microstructural evolution [23]. Ta^{+5} substitution at Fe^{+3} in BFO reduced leakage current as well as increased electrical resistivity by 6 orders of magnitude

* Corresponding author. Tel.: +1 2395374964; fax: +1 787 764 2571.
E-mail address: pvsri123@gmail.com (V.S. Puli).
[1] Presently at CICECO, University of Averio, Averio, Portugal.

0925-8388/$ – see front matter © 2011 Elsevier B.V. All rights reserved.
doi:10.1016/j.jallcom.2011.05.077

with weak ferromagnetic unsaturated hysteresis loop, where the ferromagnetic behavior is attributed to the distortion of the oxygen octahedral with tantalum (Ta) substitution [17]. Kumar and Yadav reported an increase in magnetization with increase in Ti content, in Ti substitution on $BiFe_{(1-x)}Ti_xO_3$ ceramics, prepared using rapid liquid phase sintering [24]. Magnetic properties were completely lost by Ti substitution in $BiFe_{(1-x)}Ti_xO_3$ thin films but were slightly improved with magnetically active Co co-doping [1].

In the last decade, most of the multiferroic research focuses on the characterization of the physical properties of BFO and doped BFO, but very little work has been carried out to investigate ME properties of doped BFO. The present work deals with the low temperature synthesis of BSFCO ceramics by sol–gel process, strong polarization dependent suppression of magnetic hysteresis, improved magnetization, and linear magneto-electric coupling.

2. Experimental

The BSFCO ceramics were prepared by a sol–gel route using 2 methoxyethanol and glacial acetic acid as solvents. $Bi(NO_3)_3{\cdot}5H_2O$, $Fe(NO_3)_3{\cdot}9H_2O$, $Sm(NO_3)_3{\cdot}6H_2O$ and $Co(NO_3)_2{\cdot}6H_2O$ with suitable stoichiometry were dissolved in 2 methoxyethanol and glacial acetic acid. The mixture was stirred for 2 h at 130 °C. The resulting solution was evaporated and dried at 200 °C to obtain the xerogel powder. The obtained powder was heated at 600 °C for 30 min. The phase identification was performed on a Siemen D5000, X-ray diffractometer using Cu Kα radiation (wave length 1.5405 Å) at room temperature. X-ray diffraction data were collected in wide range of Braag angle 2Θ ($20^\circ \leq 2\theta \leq 80^\circ$). For the measurement of electrical properties, the heat-treated powders were pressed into pellets (typically ~13 mm in diameter and 1.5–2 mm thick) by applying 2 ton pressure; PVA of 0.025 g/ml was also added to act as a binder during the pellet preparation process and sintered at 650 °C for 2 h. Polarization measurements were carried out using Radiant ferroelectric tester (Radiant Technologies, RT 6000 HVA-4000 Amplifier), leakage current measurements were made using Keithley 6517A electrometer/high resistance meter. The magnetization hysteresis loop (M–H loop) measurements were carried out using a vibrating sample magnetometer (VSM) (Lakeshore 7407), magneto-electric measurement by homemade probe, and ferroelectric properties of the samples were measured using a ferroelectric tester (Radiant Technology, USA).

3. Results and discussion

3.1. Crystal structure and microstructure

X-ray diffraction (XRD) patterns of the BSFCO ceramics before leaching (a) and after leaching (b) with HNO_3 and calcined at 650 °C are shown in Fig. 1(a) and (b). The prominent peaks in XRD plots are indexed to various ($h\,k\,l$) planes of BFO indicating formation of phase that exhibit similar rhombohedral perovskite structure as $BiFeO_3$. Besides these perovskite phases about 20% impurity phases, such as $Bi_2Fe_4O_9$, $Bi_{25}FeO_{40}$ were also observed in unleached BSFCO. After leaching with HNO_3 these impurity phases decreased to ~5% which in turn improved the crystal structure. XRD

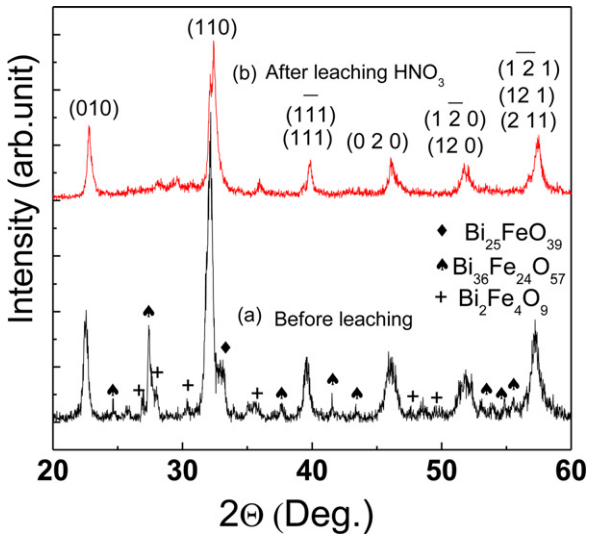

Fig. 1. . Room temperature X-ray diffraction patterns of BSFCO, (a) before leaching. (b) after leaching HNO_3.

plot of BSFCO indicates that Sm, and Co co-dopings at Bi and Fe site respective distorted the rhombohedral structure of BFO, even after leaching some impurity phases persisted. Among impurity phases the origin of extra peak at 35° is not well known. It is hard to avoid impurity phases with the co-doping of rare-earth and transition metal ions (having several valance state) in BFO like complex systems. We performed magnetic, electric, and magneto-electric measurements on BSCFO containing both high and low impurities. We found almost similar results for both the systems. Here we also present some of the characterization results of HNO_3 leached BSCFO having low impurity phases.

Fig. 2 shows the surface morphology and compositional EDX data of BSFCO from SEM picture, it revealed clusters of grains and small inhomogeneous grains on the surface with average grain size of around 500 nm to 2 μm. It is seen that the ceramics are dense without cracks. The elemental contents were estimated with EDX spectra showing Sm and Co atoms fairly incorporated into the host lattice site of $BiFeO_3$. The atomic ratio of Bi:Fe ~ 0.986 for the present samples. Nalwa and Garg [10] pointed out that if the Bi:Fe atomic ratio is greater than one, it may be due to the presence of Bi-rich secondary phases and as well as single phase nature of Sm doped BFO if the atomic ratio is ~1. The overall compositional variation on the surface is similar to the composition taken stoichiometrically.

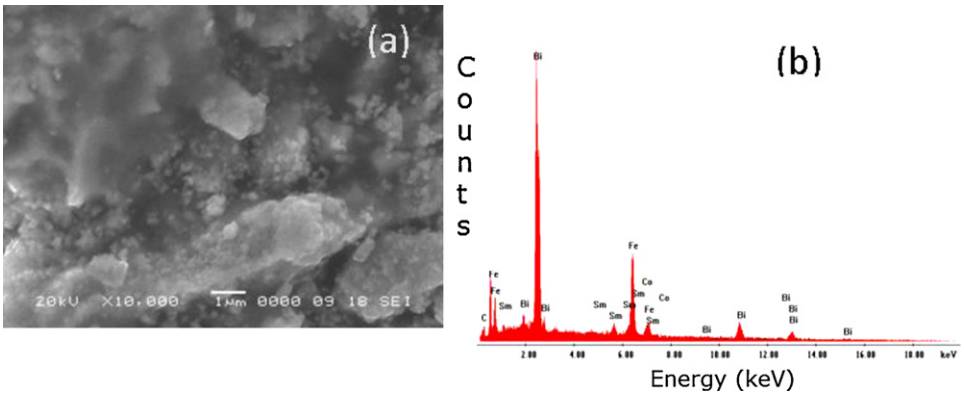

Fig. 2. . (a) SEM and (b) EDX Spectra of BSFCO for as sintered.

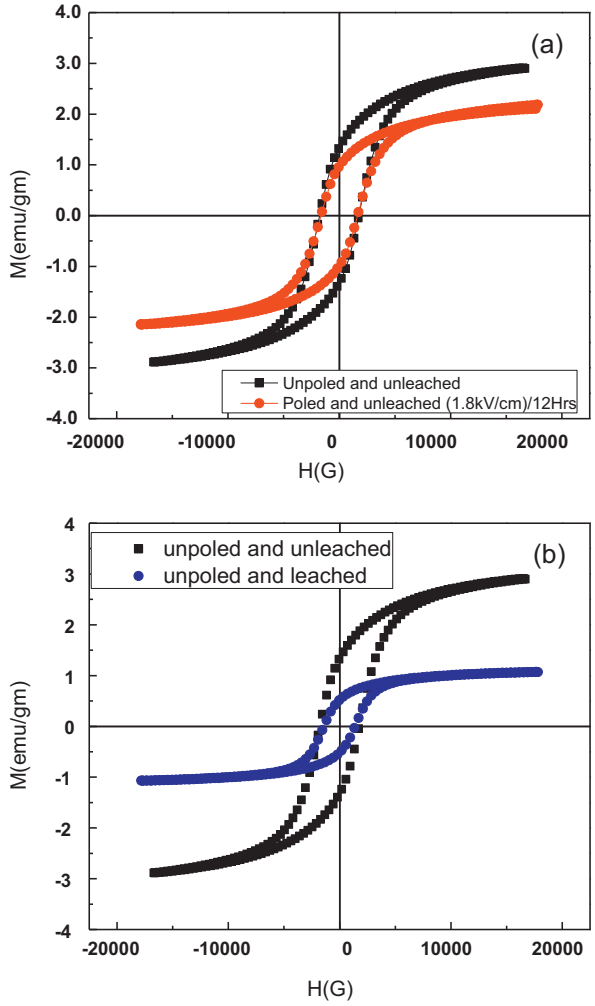

Fig. 3. (a) Magnetic hysteresis loops behavior of BSFCO for as sintered and poled under external electric field. (b) Magnetic hysteresis loops behavior of BSFCO for as sintered and leached with HNO_3 (unpoled).

3.2. Magneto-electric coupling under electrical poling

As calcined and poled Magnetization (M) vs. applied field (H) loops for BSFCO ceramics samples at room temperature were shown in Fig. 3(a). First of all, this composition showed very high magnetization compared to parent BFO, secondly, the magnetic hysteresis are well saturated with high saturation magnetization 2.89 emu/gm (unpoled and unleached) and 2.18 emu/gm (poled and unleached) respectively. Magnetization (M) vs. applied field (H) loops for BSFCO ceramics samples both unleached and leached with HNO_3 at room temperature were also shown in Fig. 3(b). Composition showed very high magnetization, and well saturated magnetic hysteresis loops, with high saturation magnetization 2.89 emu/gm (unpoled and unleached) and 1.10 emu/gm (unpoled and leached with HNO_3) respectively. Enhanced magnetization is mainly due to rare earth Sm^{3+} and transition metal Co^{3+} incorporation in to BFO. Interesting phenomena were seen after the poling of ceramics at ~1 kV/cm for 12 h, and we observed the change in saturation as well as remanent magnetization by 26%, it indicates significant amount of static magneto-electric (ME) coupling in the system. We also observe that the static ME coupling of the system was irreversible. The switching of magnetization under long time electric field slows down the spin dynamics.

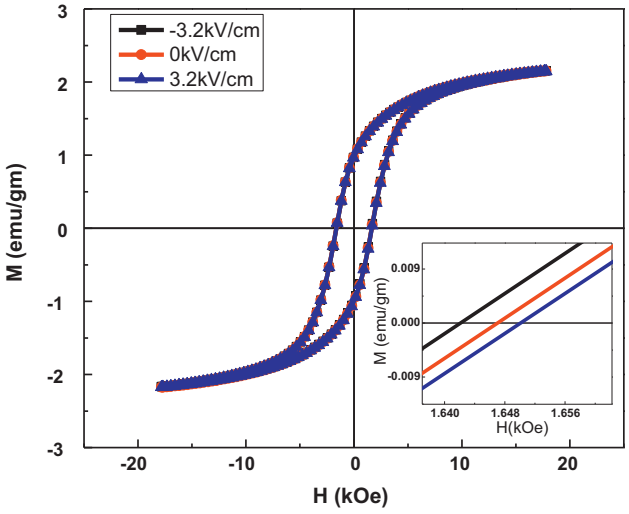

Fig. 4. . Magnetic hysteresis loops behavior for as sintered BSFCO ($E||H$) at 0, +3.2, and −3.2 kV/cm, inset shows the change in coercive field under external electric field.

3.3. Converse magneto-electric coupling

We have applied magnetic field parallel and perpendicular direction of the face of the pellets as shown in Fig. 4, in both of the cases, symmetric and well saturated hysteresis loops were obtained with coercivity (H_c) ≈ 1665 Oe and the average remanent magnetization $M_r \approx 1.04$ emu/gm and coercivity $H_c \approx 1629$ Oe for pellet

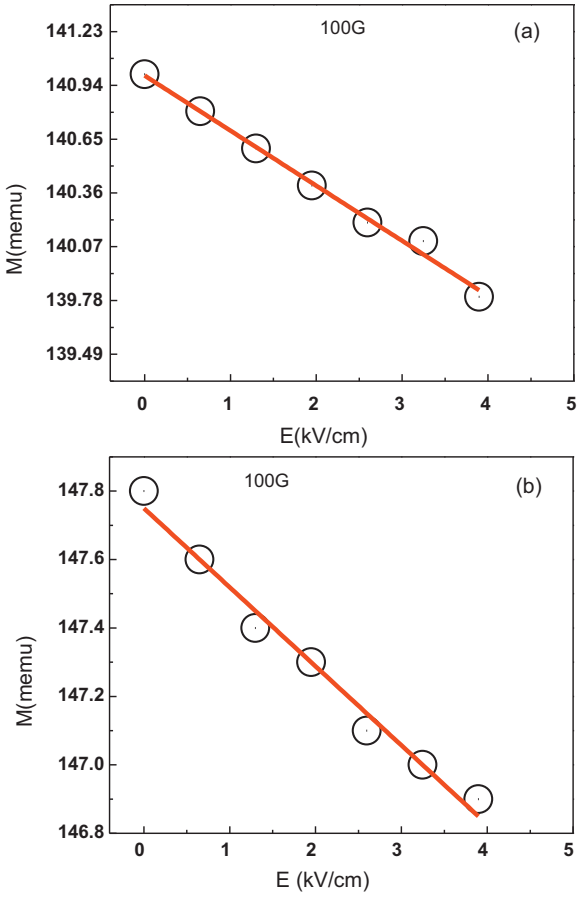

Fig. 5. . Converse ME coupling behavior of BSFCO, (a) $E||H$ and (b) $E\perp H$, measured at 100 Gauss.

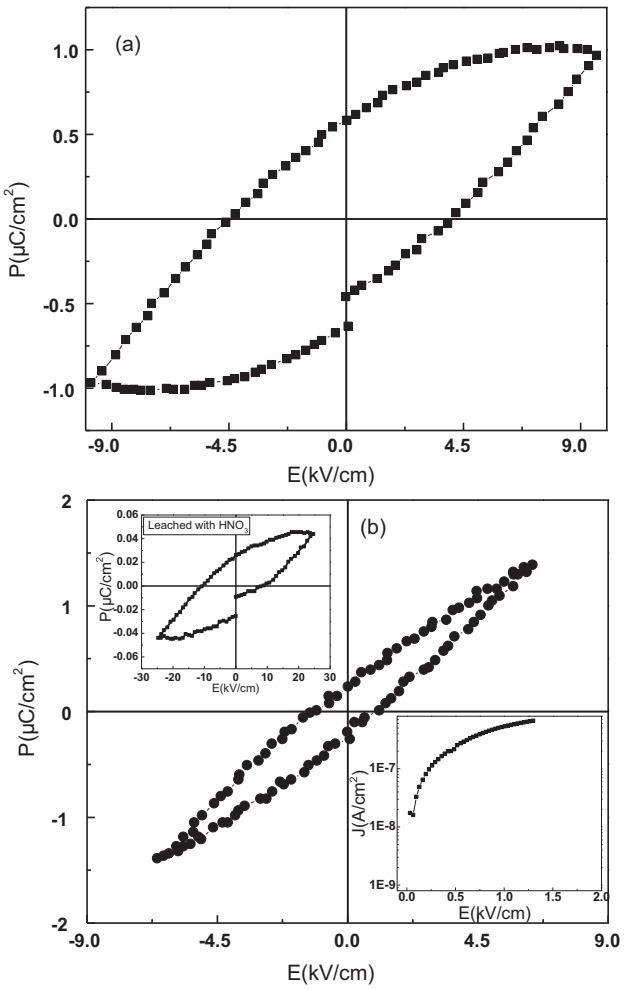

Fig. 6. . *P–E* hysteresis loops behavior of BSFCO, (a) unpoled, (b) poled (middle part—without leaching); the inset of (b) (upper part) *P–E* hysteresis loop for BSFCO unpoled and leached with HNO_3 and the inset of (b) (lower part-unleached) the dc leakage current characteristics.

face parallel to applied field, and almost similar average remanent magnetization $M_r \approx 1.03$ emu/gm for pellet face perpendicular to applied field. Larger coercivity can be attributed to Co doping at Fe site [26]. External electric field along parallel to magnetic field ($H||E$) and perpendicular to magnetic field ($H\perp E$) were applied to the pellets at fixed small magnetic field (100 Oe). Dynamic converse magneto-electric measurements were performed on poled ceramics samples. Electric field was applied along parallel and perpendicular to the magnetic field as shown in Fig. 5. Under the application of +ve and −ve external electric field, a significant amount of coercive field was changed. ME coefficients were calculated from change in magnetization (under @ 100 Oe) along parallel and perpendicular directions under applied external electric field, the calculated ME-coefficients $\alpha = \mu_0 \Delta M/\Delta E$ are ~0.8e−10 s m^{-1} and 0.6e−10 s m^{-1} respectively. The observed changes in magnetization under electric field follow linear relationship suggesting PM type of coupling as expected and observed in BFO. The present ME values are comparatively better than the value obtained for single phase Cr_2O_3 $\alpha \sim 4.1 \times 10^{-12}$ s m^{-1} [27,28] and also for other single phase materials [4,29].

3.4. Ferroelectric polarization

Polarization (P) versus Electric field (E) plots for as sintered ceramic pellets, poled @ 1.8 kV for 12 h and unpoled, leached with HNO_3 are shown in Fig. 6(a) and (b) and upper inset part of Fig. 6(b). After poling hysteresis loops become slimmer, the observed polarization values are less compare to normal ceramics or single crystal BFO. It is well known that conducting grain boundaries, presence of secondary phases, and defects make BFO ceramics conducting and very hard to get real polarization. Nowadays, with advanced growth techniques and characterization facilities are able to obtain high polarization. Our co-doped BFO is also showing the same polarization properties [3]. Yuan and Or [13], found improved ferroelectric as well as magnetic properties for A-site doping, here we have also chosen the same Sm^{+3} (ionic radius = 0.958 Å) substitution at Bi-site (ionic radius = 1.030 Å) along with Co substitution at Fe site, improved magnetization properties were obtained but still the low ferroelectric polarization and high leakage current is big concern.

The remnant polarizations (P_r) and coercive field for both unpoled (without leaching), poled samples (without leaching) and leached with HNO_3 were 0.587 μC/cm^2, 4.18 kV/cm, 0.23 μC/cm^2, 0.01 kV/cm and 0.025 μC/cm^2 2.56 kV/cm at 1500 V respectively. P_r values for the present samples are much smaller than the ceramic BFO as well as thin films prepared using sol–gel techniques [30,31]. The lower inset of Fig. 6(b), describes the dc leakage current characteristics of BCFO (without leaching) and similar results were obtained for leached samples and which were not presented here. The data shows the moderate leakage current density values that follow the mixed Schottky type and bulk limited current mechanism. We performed our ME coupling measurements well within the low leakage current region in order to avoid any experimental artifact.

4. Conclusions

In summary, Sm & Co co-substituted BFO ceramics were fabricated by sol–gel method at low sintering temperature. BSFCO exhibited distorted rhombohedral crystal structure with less than 5% impurities phase. HNO_3 leaching could reduce the impurity phase, but not much change observed in their respective properties. The poled ceramics showed 26% change in saturation and remanent magnetization under external electric field suggest significant static ME coupling. Converse ME coupling were found 0.6–0.8 × 10^{-10} s m^{-1} which is better than the single phase multiferroic obeying linear ME coupling. The *P–E* hysteresis loops are linear lossy in nature and may be due to the presence of impure phases, conducting grain boundaries and moderate leakage current. Co doping in BFO significantly improves the magnetic properties but unable to improve the polarization.

Acknowledgements

This work was supported by the Department of Energy grant # DoE FG 02-08ER46526 grants. Authors are also thankful to Cristina Diaz Borrero, Material characterization center, University of Puerto Rico for doing SEM and EDX measurements.

References

[1] N.M. Murari, R. Thomas, R.E. Melgarejo, S.P. Pavunny, R.S. Katiyar, J. Appl. Phys. 106 (2009) 014103.
[2] A. Kumar, N.M. Murari, R.S. Katiyar, Appl. Phys. Lett. 92 (2000) 152907.
[3] J. Wang, J.B. Neaton, H. Zheng, V. Nagarajan, S.B. Ogale, B. Liu, D. Viehland, V. Vaithyanathan, D.G. Schlom, U.V. Waghmare, N.A. Spaldin, K.M. Rabe, M. Wuttig, R. Ramesh, Science 299 (2003) 1719–1722.
[4] W. Eerenstein, N.D. Mathur, J.F. Scott, Nature 442 (2006) 759–765.
[5] A. Kumar, N.M. Murari, R.S. Katiyar, J. Raman Spectrosc. 39 (2008) 1262–1267.
[6] S. Shetty, V.R. Palkar, R. Pinto, Pramana: J. Phys. 58 (2002) 1027.
[7] A.V. Zalesskiĭ, A.A. Frolov, T.A. Khimich, A.A. Bush, Phys. Solid State 45 (2003) 141.
[8] F.Z. Qian, J.S. Jiang, S.Z. Guo, D.M. Jiang, W.G. Zhang, J. Magn. Magn. Mater. 322 (2010) 3127–3130.

[9] F.Z. Qian, J.S. Jiang, S.Z. Guo, D.M. Jiang, W.G. Zhang, J. Appl. Phys. 106 (2009) 084312.
[10] K.S. Nalwa, A. Garg, J. Appl. Phys. 103 (2008) 044101.
[11] M.M. Kumar, V.R. Palkar, K. Srinivas, S.V. Suryanarayan, Appl. Phys. Lett. 76 (2000) 2764.
[12] N.M. Murari, R. Thomas, A. Winterman, R.E. Melgarejo, S.P. Pavunny, R.S. Katiyar, J. Appl. Phys. 105 (2009) 084110.
[13] G.L. Yuan, S.W. Or, J. Appl. Phys. 100 (2006) 024109.
[14] V.R. Palkar, K.G. Kumara, S.K. Malik, Appl. Phys. Lett. 84 (2004) 2856.
[15] K.S. Nalwa, A. Garg, A. Upadhyaya, Mater. Lett. 62 (2008) 878.
[16] P. Uniyal, L.K. Yadav, Mater. Lett. 62 (2008) 2858.
[17] W.-S. Kim, Y.-K. Jun, K.H. Kim, S.-H. Hong, J. Magn. Magn. Mater. 321 (2009) 3262–3265.
[18] S. Vasudevan, C.N.R. Rao, A.M. Umarji, G.V.S. Rao, Mater. Res. Bull. 14 (1979) 451.
[19] I. Sosnowska, W. Schafer, I.O. Troyanchuk, Physica B 276–278 (2000) 576.
[20] K. Takahashi, M. Tonouchi, J. Magn. Magn. Mater. 310 (2007) 1174.
[21] M. Azuma, H. Kanda, A.A. Belik, Y. Shimakawa, M. Takano, J. Magn. Magn. Mater. 310 (2007) 1177.
[22] S.R. Shannigrahi, A. Huang, D. Tripathy, A.O. Adeyeye, J. Magn. Magn. Mater. 320 (2007) 2215.
[23] S.R. Das, P. Bhattacharya, R.N.P. Choudhary, R.S. Katiyar, J. Appl. Phys. 99 (2006) 066107.
[24] M. Kumar, K.L. Yadav, Appl. Phys. Lett. 91 (2007) 112911.
[25] Q. Xu, H. Zai, D. Wu, T. Qiu, M.X. Xu, Appl. Phys. Lett. 95 (2009) 112510.
[26] H. Naganuma, J. Miura, S. Okamura, Appl. Phys. Lett. 93 (2008) 052901.
[27] D.N. Astrov, Zh. Eksp. Teor. Fiz. 38 (1960) 984–985;
D.N. Astrov, Sov. Phys. JETP 11 (1960) 708–709.
[28] V.J. Folen, G.T. Rado, E.W. Stalder, Phys. Rev. Lett. 6 (1961) 607–608.
[29] W.F. Brown Jr., R.M. Hornreich, S. Shtrikman, Phys. Rev. 168 (1968) 574–577.
[30] M.S. Awan, A.S. Bhatti, J. Mater. Eng. Perform., ASM International, 20 (2) (2010), pp. 1059–9495.
[31] Dong Hong, Shengwen Yu, Jinrong Cheng, Current Appl. Phys. (2011), in press, doi:10.1016/j.cap.2011.01.029.